Cancer Letters 453 (2019) 131–141

Contents lists available at ScienceDirect

Cancer Letters

journal homepage: www.elsevier.com/locate/canlet

Original Articles

The TLK1-Nek1 axis promotes prostate cancer progression

Vibha Singh[a], Praveen Kumar Jaiswal[a,1], Ishita Ghosh[a,1], Hari K. Koul[a,b,c], Xiuping Yu[a], Arrigo De Benedetti[a,*]

[a] Department of Biochemistry and Molecular Biology, Louisiana State University Health Sciences Center, Shreveport, USA
[b] Feist Weiller Cancer Center, USA
[c] Overton Brooks VA Medical Center, Shreveport, USA

ARTICLE INFO

Keywords:
Tousled like kinase (TLK)
NIMA related kinase 1 (Nek1)
DNA damage response (DDR)
Androgen deprivation therapy (ADT)
Castration
Thioridazine (THD)

ABSTRACT

We recently uncovered the critical TLK1 > NEK1 > ATR > Chk1 axis in mediating the DDR and cell cycle checkpoint while transiting from Androgen Sensitive to Insensitive growth for LNCaP and TRAMP-C2 cells. However, we did not know the generality of this pathway in PCa progression since there are few cell lines where the transition has been studied. Furthermore, the identification of Nek1, and more importantly the TLK-mediated phosphorylation of T141, has never been studied in PCa biopsies. We now report the first study of a PCa TMA of p-Nek1-T141 and correlation to the Gleason score. In addition we found that TRAMP mice treated with the TLK inhibitor, thioridazine (THD), following castration did not recover cancerous growth of their prostates. Moreover, we recapitulated the process of translational increase in TLK1B expression in a naïve PDX model that was established from an AR + adenocarcinoma. Therefore, we believe that this TLK1-Nek1 mediated DDR axis is likely to be a common adaptive response during the transition of PCa cells toward androgen-insensitive growth, and hence CRPC progression, which has the potential to be targeted with THD and other TLK or Nek1 inhibitors.

1. Introduction

Standard therapy for Prostate Cancer (PCa) that has progressed beyond localized treatment control consists of androgen-deprivation therapy (ADT) which provide respite from disease progression, but ultimately fail resulting in the incurable phase of the disease: mCRPC. Targeting PCa cells before their progression to mCRPC would greatly improve the outcome. An important area of clinical work is how to target the DNA Damage Response (DDR) to kill the cancer cells, but this has been limited by general toxicity of checkpoint inhibitors, and much effort is being devoted to finding specific cancer cells' molecular targets. We have recently uncovered in two Androgen Sensitive (AS) lines – LNCaP and TRAMP-C2 – that androgen deprivation results in a temporary cell cycle arrest that protects the cancer cells from dividing with damaged DNA, and have uncovered the likely signal transduction pathway that in brief follows this pattern: ADT > mTOR > TLK1 > Nek1 > ATR > Chk1 [1]. In the rapid first step following ADT, TLK1 is translationally upregulated via the compensatory mTOR > 4EBP1 pathway [2], thereby initiating the DDR cascade that results in the cell cycle arrest. Abrogation of the DDR via adding the specific TLK inhibitor, thioridazine (THD), results in accumulation of DNA damage and DSBs that eventually lead to apoptosis, thereby preventing the progression of AS cells toward the Androgen Independent (AI) growth, both in vitro and in xenografts of LNCaP cells. In fact, tumor growth was suppressed by the combination treatment of bicalutamide plus THD. However, this work was largely mechanistic and insufficiently generalized, as only the LNCaP model, and partly the TRAMP-C2 models were used in that study. We now set up to confirm this in two more models, including a PDX and the TRAMP mice, as well as in a tissue microarray (TMA) study the generality of the TLK1-Nek1 axis as one of the earliest events during the process of adaptation of PCa cells to ADT. We further show that this is a step that can be optimally targeted in the clinics by adding specific inhibitors of TLKs, like THD, to the standard of care for advanced PCa (ADT).

2. Materials and methods

Analysis of the PCa-TMA. IRB approval was obtained for the use of the TMA, and the TMA was obtained with Informed Consent and following The Code of Ethics of the World Medical Association. TMA block

* Corresponding author.
E-mail addresses: vsing2@lsuhsc.edu (V. Singh), pjaisw@lsuhsc.edu (P.K. Jaiswal), ighosh@lsuhsc.edu (I. Ghosh), hkoul@lsuhsc.edu (H.K. Koul), xyu@lsuhsc.edu (X. Yu), adeben@lsuhsc.edu (A. De Benedetti).
[1] Equal co-contributors.

https://doi.org/10.1016/j.canlet.2019.03.041
Received 13 March 2019; Received in revised form 21 March 2019; Accepted 22 March 2019

of prostate cancer FFPE tissues was built using the Galileo CK4500 semiautomatic Tissue Microarrayer (ISENET-USA LLC, Philadelphia, USA) per manufacturer's protocol. 34 cancer and 1 benign prostate blocks were cored with a 1.0 mm core needle in triplicate. 2 Additional cores that contained only normal prostate tissue that was adjacent to PCa areas were also included. The layout was set to 12 columns by 9 rows with the first set of triplicate cores left intentionally blank for orientation purposes. Sectioning and processing of the tissues were carried out in the FWCC Histology Service, using automated processes and equipment to provide uniform and standardized results. IHC staining for this TMA and the TRAMP prostate tissues was as described in Ref. [3]. Representative IHC images were taken at ×40 magnification with an Olympus B×51 microscope. Positive staining were quantified by NIH ImageJ software with an average of three fields. 2-way ANOVA analysis was carried to compare the intensity of staining.

Animal use. All animals used in this study received humane care based on guidelines set by the American Veterinary, and approved by the Institutional Animal Care and Use Committee of LSU Health Sciences Center at Shreveport. All animal experiments were also approved by the DoD-ACURO and fully complied with the ARRIVE guidelines. 12-week-old TRAMP mice were used to observe PIN regions. We used ~16 weeks old TRAMP mice and treated with 9 dose of THD (10 mg/kg/body weight). In another set of experiment, ~20 weeks old TRAMP mice were castrated and treated with 9 dose of THD (10 mg/kg/body weight). Whole GU was collected, weighted and fixed in 4% formalin for further processing of tissues. The NSG-TM00298 PDX model was purchased from the Jackson laboratory, and propagated in 6 SCID mice until the tumors grew to ~1000 mm^3. Two mice were then treated with Bic on alternate days for one week, after which all the mice were sacrificed and the tumor isolated for protein and RNA analysis.

2.1. Cell lines

The TRAMP-C2 cell line was recently purchased from the ATCC and cultured according to their guidelines. Analysis of cell cycle by PI staining was carried out as described in Ref. [4].

2.2. List of antibodies

TLK1 antibody [N2C2], Internal-Genetex- Cat. #GTX102891.
pNek1 antibody - Purified custom - Thermofisher Scientific/Pierce.
Anti-Phospho-Histone H2A.X (Ser139) – Millipore–Cat. #05-636.
Cleaved Caspase-3 (Asp175) (D3E9) - CST-Cat. #9579.
Cleaved PARP (Asp214) (D64E10) Rabbit mAb CST-Cat. #5625.
Chr-A Antibody (C-12) Santa Cruz Cat. #393941.
Ki-67 (D3B5) Rabbit mAb – Cell Signaling - Cat #12202.
Alpha –rabbit IgG-HRP – CST-Cat.# 7074S.
Alpha -mouse IgG-HRP CST-Cat.# 7076.
Anti-beta Tubulin antibody - Loading Control (HRP)-Abcam- Cat.# (ab21058).
Tubulin Antibody (2-28-33) -Loading Control HRP Santa Cruz Cat.# −23949 HRP.

2.3. Cell cycle analysis

Tramp C2 cells were seeded in 6-well plates at a density of 2×10^5 cells/well and treated. The next day cells were treated for one day with Biacalutamide and THD at 10 μM. Cells were washed with 1X PBS and trypsinized, washed twice in ice-cold 1X-PBS and fixed in 70% ethanol overnight. Samples were then stained with Propidium Iodine 50 μg/ml (Sigma Aldrich P4170, 3.8 mM Sodium Citrate and 0.5 μg/ml RNase A. Samples were then imperiled to FACS Calibur flow cytometer (Becton–Dickinson). Quantitative amounts of cell cycle phases (G1, S, G2, M) were determined by FACSDiva and Modfit modeling software.

2.4. Western blot analysis

Cells were lysed in 1X SDS sample buffer. Lysates were sonicated for 15 s and heated at 100 °C for 5 min. Proteins were separated on 6–12% SDS-PAGE gels and transferred to PVDF membranes (Millipore). Membranes were incubated with PBS containing 0.05% Tween 20 and 5% non-fat dry milk to block non-specific binding and were incubated with primary antibodies; membranes were then incubated with appropriate secondary antibodies conjugated to horseradish peroxidase. Immunoreactive bands were visualized using chemiluminescence reagent.

2.5. Quantification of the TLK1B mRNA expression in PDX

Total RNA was extracted from ~10 mg of tumor tissue using the QIAGEN RNeasy MiniKit. The cDNA synthesis and analysis was carried out as described in Ref. [1].

3. Results

Nek1-T141 phosphorylation increases with prostate cancer stage in primary biopsies of untreated patients. We recently reported a C-Bioportal analysis of Nek1 that revealed upregulation in 33% of patients and gene amplification in 12% of patients with CRPC-Neuroendocrine Prostate Cancer (NEPC, a type of AR negative CRPC). Moreover, Nek1 mRNA is upregulated in 21% of patients with metastatic PCa. This may implicate a function of Nek1 in PCa progression. However, this must be only part of the story because Nek1 is conformationally constrained in inactive state by an activation loop [3]. And we previously reported that TLK1 phosphorylates T141 that lies adjacent the activation loop, leading to its activation [4]. So that the phosphorylation status of Nek1-T141 is really the more critical information that we set to study in order to uncover the real significance of Nek1 in PCa progression. For this, we analyzed a TMA generated by the department of Pathology and the FWCC at LSUHSC that contained 35 PCa biopsies, one benign sample (BPH), and two cancer-free tissues in two patients that also had a cancer-positive biopsy, arranged by tumor stage and Gleason Score (GS). We previously showed that the p-Nek1affinity-purified antiserum we have generated is highly specific (does not react with Nek1-T141A mutant) and is suitable for IHC [1]. Our TMA analysis by IHC revealed that p-Nek1-T141 was elevated in tumor biopsies compared to the normal specimens (***$p < 0.001$), and that the intensity of staining correlated with the GS and tumor stage (GS7 ***$p < 0.001$, GS8 **$p < 0.01$), and where staining was weaker in the stroma and most elevated in the luminal cancer cells niches (Fig. 1A–C). Note that a pan-Nek1 antiserum we have purchased from Bethyl labs is not suitable for IHC analysis of FFPE samples, so that we cannot rule out that there was an increase in total Nek1.

The p-Nek1 staining correlates with the expression of TLK1B. We previously showed that the TLKs are likely the only kinases that phosphorylate Nek1-T141, since overexpression of several dominant negative mutants of TLK1B suppressed Nek1 phosphorylation (judged by mobility on SDS/PAGE [4]), while subsequently we showed that the addition of the specific TLK inhibitor, THD, specifically suppressed the phosphorylation of T141 [1]. Notably, the TLK1 gene was identified by co-expression analysis using WGCNA as a key driver of PCa [5], so it seemed quite possible that the increased p-Nek1 could be in part a consequence of the GS-stage related increase in TLK1B expression, and therefore that there should be a correlation between TLK1B expression and p-Nek1 This expectation was partially met since in GS8 samples the intensity of TLK1B and p-Nek1 was maximally elevated and well correlated. The difference in staining between the normal sample and the cancer samples is significant (**$p < 0.01$), and correlated with GS (GS7 **$p < 0.01$, GS8 *$p < 0.05$). However, we should note that there was not much difference between GS6 and GS7 for TLK1B, whereas p-Nek1 was increased in those samples (Fig. 1D–F).

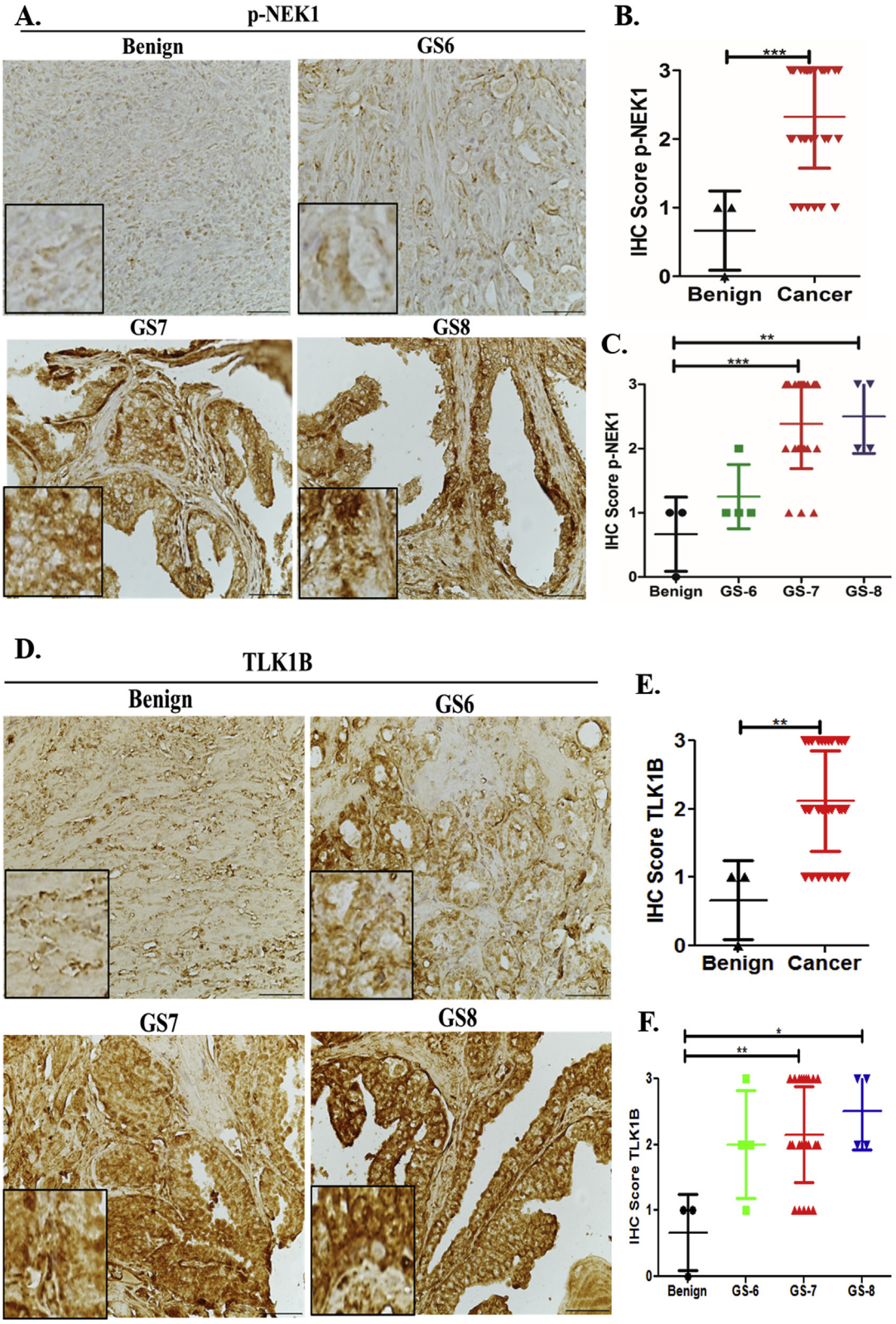

Fig. 1. A) TMA IHC analysis of phopho-Nek1-T141 (p-Nek1) is elevated in PCa in comparison to a BPH lesion and normal prostate tissue, and the staining correlates with the Gleason Score (GS). B) The expression of TLK1B increase in PCa compared to BPH and correlates with GS.

In TRAMP mice the progression to PCa correlates with increased p-Nek1 and TLK1 expression. In TRAMP mice, expression of the PB-Tag is restricted to lobes of the prostate and the temporal pattern of transgene expression correlates with sexual maturity. TRAMP mice display high grade PIN and/or well-differentiated prostate cancer by 10–12 weeks of age. Ultimately, TRAMP mice spontaneously develop invasive primary adenocarcinomas that involves most of the prostate and greatly increases its weight. Later on the cancer cells routinely metastasize to the lymph nodes and lungs [5]. Early castration (12 weeks) results in a decrease in tumor volume burden, but ultimately has

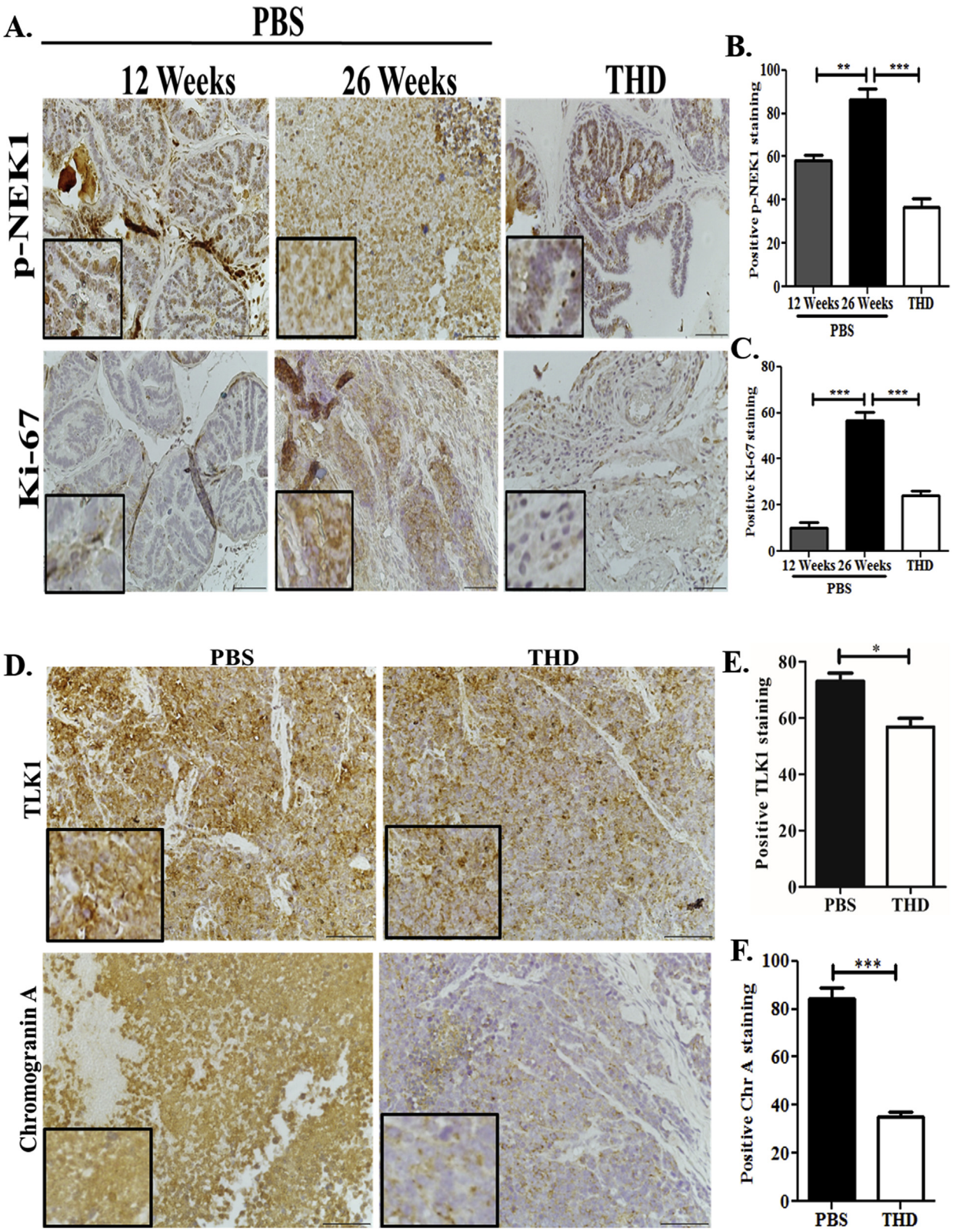

Fig. 2. IHC analysis of PCa progression in the TRAMP model. A-C) The phosphorylation of Nek1-T141 is evident by 12 weeks of age when PIN lesions begin to develop, and can be suppressed by systemic treatment with THD. In addition, the proliferative index, indicated by the % of Ki67-positive cells, can be reduced by THD treatment in 26 weeks-old mice. D-E) The expression of TLK1 is highly elevated in prostate cancer tissue from 30 weeks-old mice, but THD treatment decreases progression to NE lesions, as indicated by suppression of chromogranin staining.

no effect on time and progression to mCRPC [6], thus creating an opportunity to identify molecular targets and therapies relevant to delay or prevent progression to PCa development and later to CRPC. We thus set out to determine at 12 weeks vs. 26 weeks of age the status of p-Nek1. A group of mice were also treated with THD (inhibitor of TLKs and hence p-Nek1) to determine if this could delay cancer progression. Representative samples are shown in Fig. 2A and the quantitation in Fig. 2B (p-NEK1, PBS 12 week vs PBS 26 week, **p < 0.01). At 12 weeks, there was clear evidence of hyperproliferation of the gland and possibly evidence of PIN formation, but the cells remained nested in clearly defined acini with no evidence of stromal invasion. Ki67, a maker of proliferation, gave weak staining indicating the low level of hyperproliferation of these lesions (Fig. 2A lower panel and the quantitation Fig. 2C (Ki-67, PBS 12 week vs PBS 26 week, ***p < 0.001). In contrast, at 26 weeks, there was clear evidence of extensive cancer spread of the lobe and invasion. Correspondingly, p-Nek1 was significantly increased both in the number of cells involved and intensity. Ki67 was likewise greatly increased. In contrast, in the group of mice that were treated with THD starting at 16 weeks, two effects were obvious: 1) the phosphorylation of Nek1 was almost completely suppressed, as one would expect from the inhibition of TLK activity. 2) There was little progression from the confined PIN (or early adenocarcinomas) to the highly invasive profile seen at 26 weeks. Similarly, Ki67 staining was much weaker indicating the low proliferative characteristics of these lesions in THD-treated mice (Fig. 2B, D, 26 week PBS vs THD***p < 0.001 for P-NEK1 and Ki-67). However, in other mice treated with THD there was progression to invasive adenocarcinomas around 28 weeks of age, indicating that THD alone does not prevent eventual progression to PCa in the TRAMP model.

THD treatment of TRAMP mice decreases progression to NE lesions. The pathobiology of TRAMP mice is that poorly differentiated tumors arising in > 28-week-old mice, or at a higher frequency in castrates, express neuroendocrine markers such as chromogranin-A and synaptophysin [6]. Indeed, around 28 weeks in the TRAMP model the PCa cells convert from AR-dependent adenocarcinomas to a AR-negative neuroendocrine (NE) phenotype, which is considered a more aggressive, less treatable form of the disease in humans. At 30 weeks, there was clearly evidence of invasive cancer spread in the prostate (Fig. 2). Moreover, treatment of mice with THD did not alter much the expression of TLK1 (Fig. 2D and E, *p < 0.05), as would be expected since THD only affects the activity of TLK1 and generally not its level. However, Nek1 would not be phosphorylated in the THD treated mice, and we found that this greatly affected the NE differentiation. Whereas, the tumors from the untreated mice show strong chromogranin-A staining, the tumors from THD-treated mice showed very few cells that were stained (Fig. 2D and E, ***p < 0.001). Interestingly, as stated above, Nek1 expression was found to be elevated in a significant proportion of human NE-PCa, but the TRAMP model described here is the first evidence that p-Nek1 may be important for NE differentiation around 28 weeks of age.

The TLK1 (mouse or TLK1B in human) > Nek1 > ATR DDR axis is conserved in all ADT PCa models tested. We previously proposed that spontaneous damage from replication stress in growing PCa tumors results in frequent activation of the DDR via the ATR > Chk1 pathway, and in fact we have shown strong presence of pATR in subcutaneous LNCaP tumors of control mice, while mice treated with THD showed suppression of pATR via inhibition of the TLK1 > Nek1 > ATR DDR pathway [1]. In fact, the suppression of pATR correlated with suppression of p-Nek1 by THD. However, we needed to verify that a similar suppression of p-Nek1 (via inhibition of TLK activity) was seen in 20 weeks-old mice treated for the last four weeks with THD, similar to the experiment analyzed in Fig. 1 by IHC. To obtain a more quantitative result, the tumors-containing prostates of control mice vs. mice treated with THD were homogenized and analyzed by western blots (Fig. 3A). The prostates from all 3 control mice showed similar levels pNek1, whereas the mice treated with THD showed complete suppression of Nek1-T141 phosphorylation. Conversely, we have previously showed that ADT results in a rapid mTOR-dependent increase in TLK1 expression and a corresponding increase in Nek1 phosphorylation, which is one of its main substrates [1,4]. And in fact, castration of all 3 TRAMP mice tested resulted in increased p-Nek1 (Fig. 3B) in parallel with increased TLK1 expression that was seen in all castrated mice we have analyzed (by IHC - Fig. 5), and as previously shown also for the TRAMP-derived cell line, TRAMP-C2 [1]. We wanted to confirm the generality of this pathway also in an additional primary human PDX model from an AR-expressing adenocarcinoma: NSG-TM00298. SCID mice were implanted subcutaneously with the PDX, and after the tumors grew to ~1000 mm^3, two mice were left untreated while two received Bicalutamide (Bic) twice in one week prior to sacrifice and excision of the tumors. As anticipated, the expression of TLK1B was strongly increased in the Bic-treated mice (Fig. 3C), and correspondingly there was a strong increase in p-Nek1 (Fig. 3D). Analysis of the expression of the TLK1B splice variant by qRT-PCR revealed a ~50% reduction in TLK1B mRNA (P = 0.01) in PDX tumors isolated from mice treated with BiC compared to those untreated (Fig. 3E), supporting the idea that the mechanism of TLK1B upregulation is most likely at the translation level following activation of the mTOR > 4EBP1 axis [2].

THD treatment of TRAMP mice results in slower prostate cancer progression by increasing DNA damage and frequency of apoptosis. We previously reported that treatment of LNCaP cells with Bic or charcoal-stripped serum results in a rapid increase in TLK1B expression and the parallel activation of the DDR via the Nek1 > ATR > Chk1 pathway, and resulting in a well-known G1/S cell cycle arrest prior to their latter conversion to AI-growth [1]. Suppression of this protective DDR-induced arrest, with concomitant THD treatment, resulted in bypass of G1/S arrest and subsequent mitotically-generated DSBs and induction of apoptosis. We have now confirmed the same results with the TRAMP-derived C2 model, wherein the combined Bic + THD treatment resulted in a 30% fraction of apoptotic cells (Fig. 3F; sub-G0). To determine if a similar effect was seen during progression of TRAMP PCa tumors, mice were sacrificed at 20 weeks following four weeks of treatment with THD. We hypothesized that suppression of the DDR by inhibition of p-Nek1 with THD could result in increased unrepaired DNA damage and hence greater apoptotic response. Indeed, THD treatment resulted in increased staining for γ-H2AX (both intensity and proportion of cells), as well as staining for cleaved Caspase 3 and PARP, which are indicators of presence of DSBs and of apoptotic cells, respectively (Fig. 4A–C, PBS vs THD***p < 0.001).

Combination of castration and THD suppresses the resumption of PCa growth, CRPC progression, and results in elevated apoptotic markers in prostate tumors. When TRAMP mice are castrated at about 20 weeks of age there is a temporary suppression of PCa progression and in fact some regression of their prostates' volumes. But by 28 weeks their PCa tumors have all resumed growth and become terminal in size (humane end-point). At that time, most tumors have converted to NE type and there are frequent metastases. However, we reasoned that concomitant treatment with castration, resulting in increased TLK1 expression, and THD to suppress the TLK1 > Nek1 DDR axis, would result instead in increased apoptosis and hence restrain of PCa tumor growth/progression. Therefore, we castrated a group of 20–21 weeks old mice, and then further treated one-half with THD for four weeks. One week after the end of treatment the mice were sacrificed for analysis of their prostates. As shown in Fig. 5A–C, the prostates from many control and castrated mice had reached the terminal growth point of 4–6 gr and completely filled with cancer cells, although the prostates from 3 castrated mice still showed the initial decrease in size (regression) compared to the weight of the prostates of untreated mice. In contrast, most mice that received THD in addition to castration showed generally small prostates that on appearance had still overall normal morphology (Fig. 5A). The prostates of mice that were left untreated (PBS) compared to those treated with THD (but no

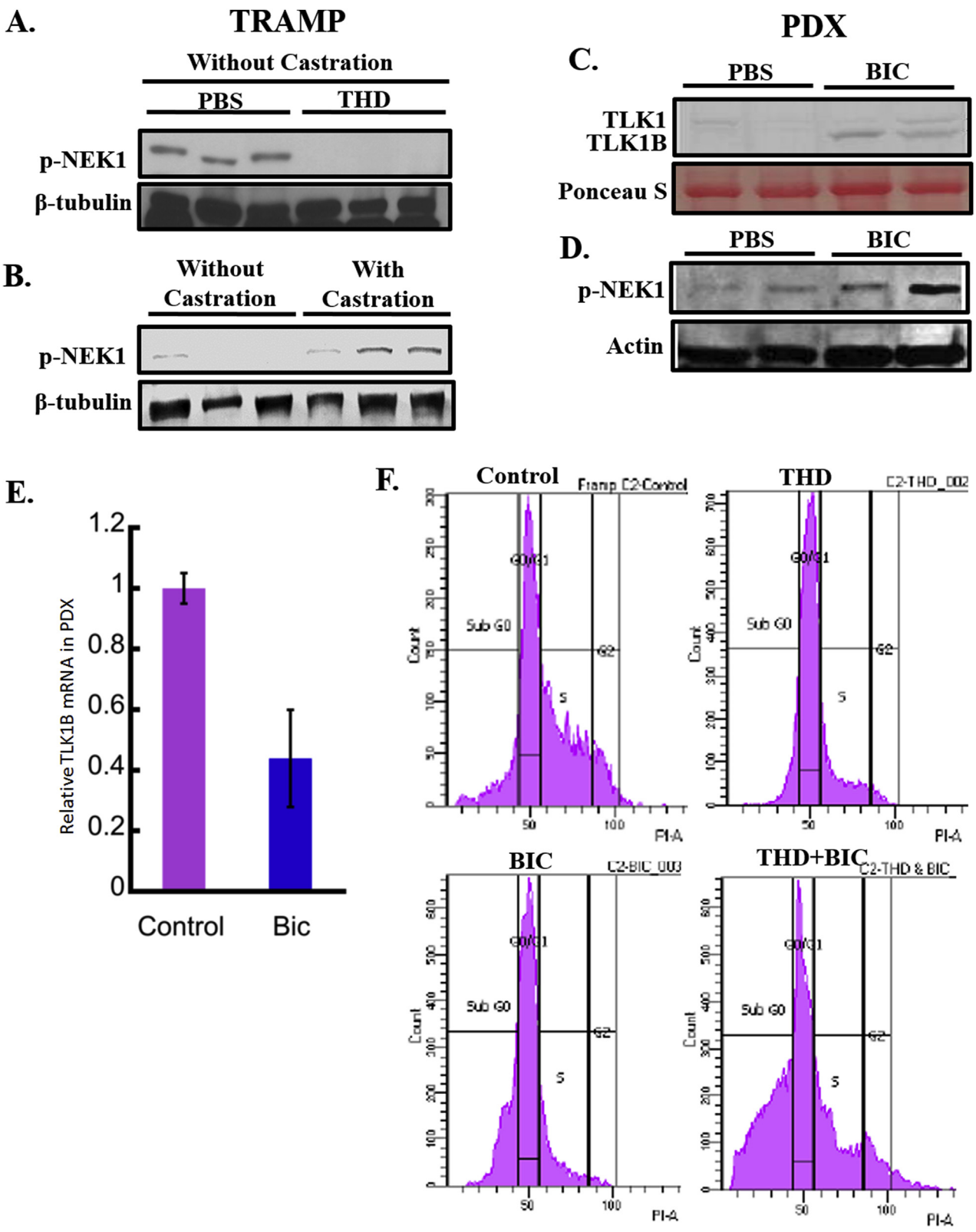

Fig. 3. A, B) WB analysis of p-Nek1 in a group of 20 weeks-old mice that have been treated with THD for 1 month (A) or one week following castration. C, D) WB analysis of TLK1B expression and P-Nek1 in the PDX model NSG-TM00298, without or with treatment with Bicalutamide (Bic), one bi-weekly dose. E) The expression of TLK1B mRNA, which was slightly reduced in the PDX mice treated with Bic (n = 4 tumors), does not correlate with the increased TLK1B protein expression. F) Treatment of TRAMP-derived C2 cells with ADT + THD results in apoptosis. TRAMP-C2 cells were incubated bicalutamide (10 μM), THD (10 μM), or bicalutamide + THD for 24 h before cell cycle analysis of PI-stained cells. Note the ~30% fraction of Sub-G0 cells in the combination treatment. Note also that whereas Bic induced a G1 cell cycle arrest with loss of the G2 population, concomitant treatment with THD prevented this, as shown by the presence of cells in S and G2.

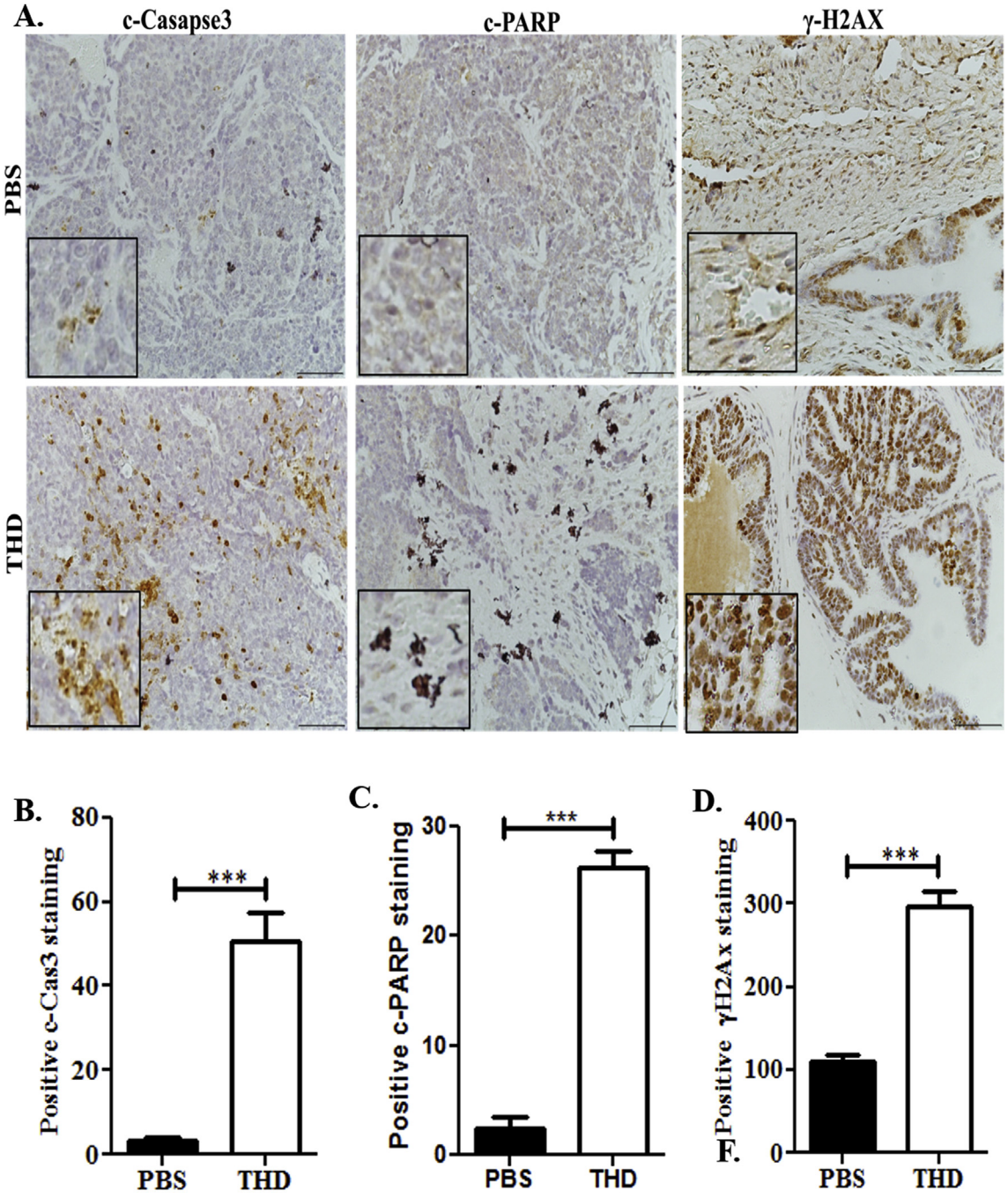

Fig. 4. THD treatment of TRAMP mice results in slower prostate cancer progression by increasing DNA damage and frequency of apoptosis. A) representative images of 26-old mice treated with THD or vehicle (PBS) showing that THD resulted in increased staining for γ-H2AX (both intensity and proportion of cells), as well as staining for cleaved Caspase 3 and PARP. B-D) Quantitations of the IHC analyses for cleaved Caspase 3 and PARP and for γ-H2AX.

castration) were similarly on average 2 gr in size, whereas those of mice that were treated with THD following castration were almost invariably regressed (~1 gr) and clearly different from most mice that were only castrated. IHC representative examples are shown in Fig. 5D and E for p-Nek1, TLK1 and Ki67. As expected, castration (ADT) resulted in increased expression of TLK1, while follow-up treatment with THD did not change this. In contrast, castration resulted in a strong increase in p-Nek1 (compare also with Fig. 1-PBS-26 weeks), whereas castration followed by THD strongly suppressed p-Nek1 (Fig. 5D and E; PBS vs THD $^{**}p < 0.01$). Cumulative evidence suggests that proliferating AS-cells are induced to undergo apoptosis by concomitant ADT + THD treatment, and consistent with this, there was a marked reduction in Ki67 (a marker of proliferating cells) staining in mice treated with THD following castration (Fig. 5D and G; PBS vs THD $^{***}p < 0.001$). To confirm that the combination of castration followed by THD results in induction of apoptosis during resumption of prostates' tumor growth at the onset of CRPC progression, we analyzed by IHC for the presence of cleaved Caspase 3 and PARP for apoptotic cells and of γ-H2AX for DSBs. Staining for all 3 markers was highly increased in castrated mice treated with THD compared to mice that were only castrated (PBS group), as shown in Fig. 6 (A-D; PBS vs THD $^{***}p < 0.001$). This is consistent with our model that treatment with THD in combination with ADT results in bypass of the DDR and hence induction of apoptosis.

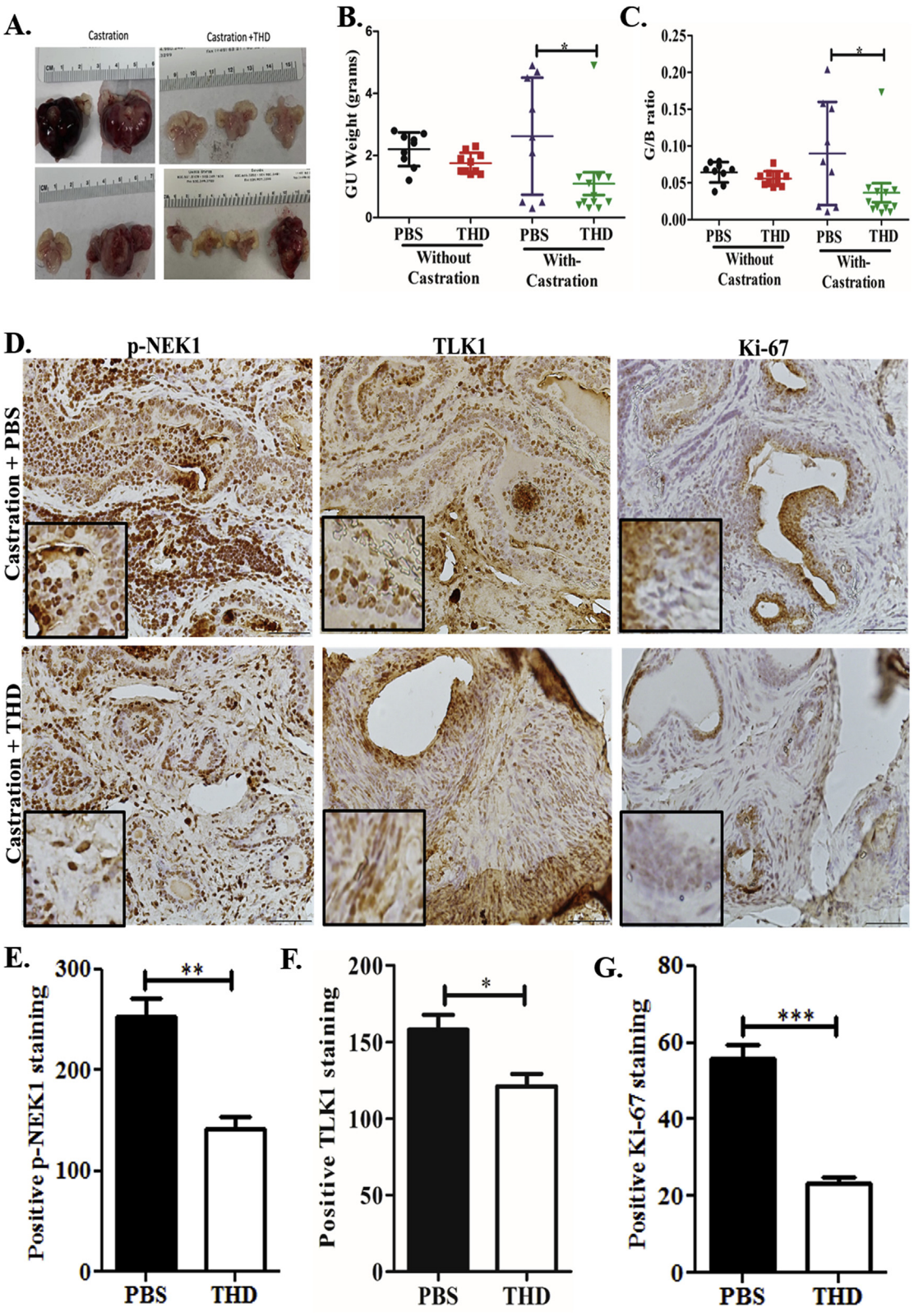

Fig. 5. A-C) Representative images of prostates and their weights in ~28-weeks old mice castrated at 20–21 weeks and treated or not with THD for 4 weeks, prior to sacrifice one week later. D-E) Representative IHCs stained for P-Nek1, TLK1 and Ki67 from the same animals. Note the reduction in P-Nek1 and Ki67 staining in the mice that were treated with THD.

4. Discussion

The Tousled Like kinases (TLK1 and TLK2) function in several processes including chromatin assembly, replication, transcription, DNA repair, and chromosome segregation (rev. in Refs. [7,8]). Expression of TLKs is frequently elevated in cancer and correlates with malignancy, prognosis and response to therapy [9,10], while their inhibition or suppression of expression sensitizes cancer cells to DNA

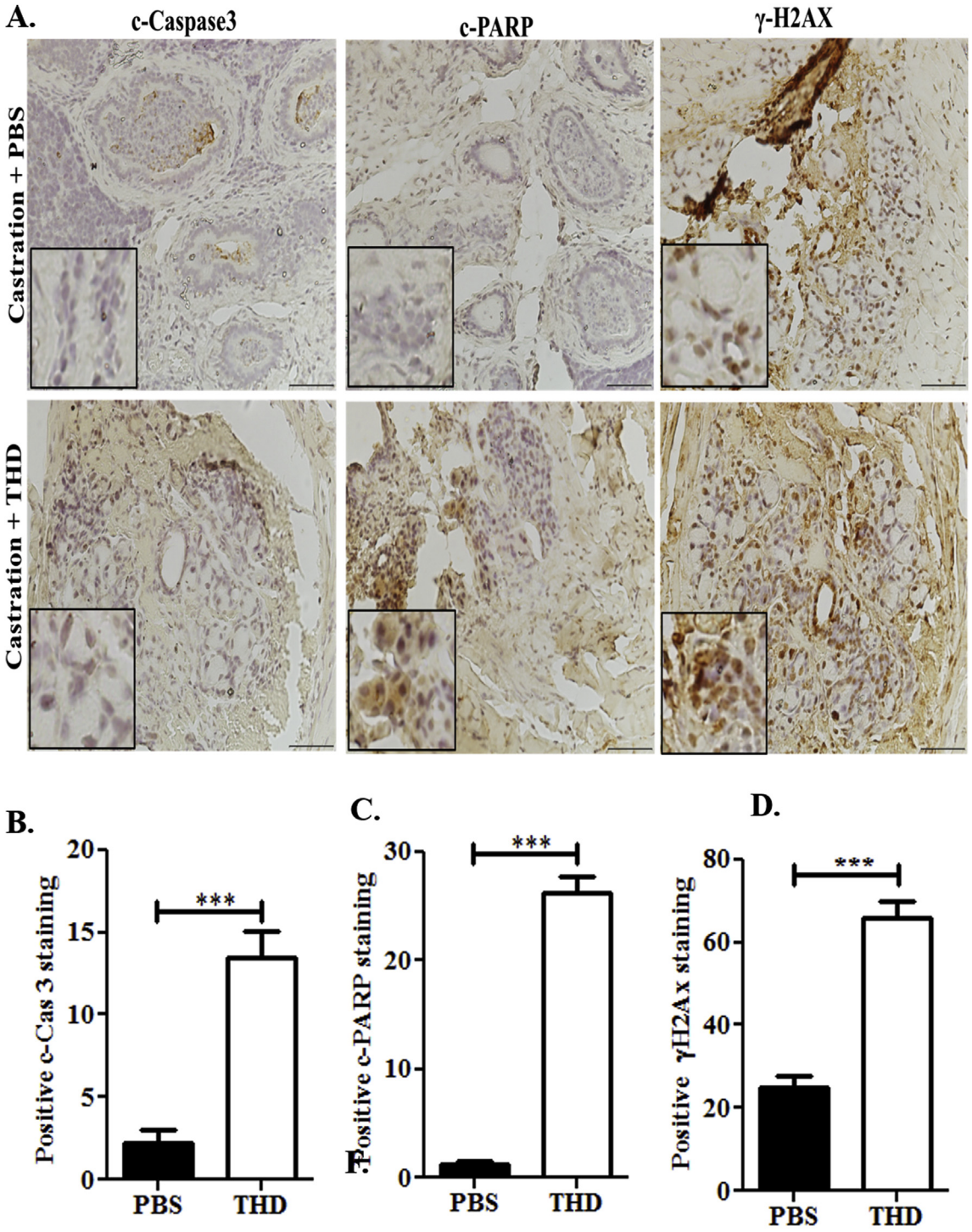

Fig. 6. A) Combination of castration and THD suppresses the resumption of PCa growth and results in elevated apoptotic markers in prostate tumors. Representative IHCs stained for cleaved Caspase 3 and PARP and for γ-H2AX. Note the significantly elevated staining for these markers in the mice treated with THD, which is quantitated in (B–D).

damaging agents [11] or PARP inhibitors that diminish repair [10]. Notably, the TLK1 gene was identified by co-expression analysis using WGCNA as a key driver of PCa, highly enriched among candidate genes collected from expression Quantitative Trait Loci (eQTL), somatic copy number alterations (SCNA), and prognostic analyses [12], and the expression of TLK1B was found elevated in several PCa cell lines in comparison to RWPE1 normal prostate line [13]. Expression of TLKs appears to be controlled at both transcription and translation levels [10,14,15] and the human splice variant TLK1B is particularly dependent on the mTOR-4EBP1-eIF4E pathway [14], a nexus which is frequently upregulated in cancer [16,17] and constitutes a key therapeutic target [18]. Recently we have identified the proteome complement of TLK1/1B, and have identified the protein kinase Nek1 as one of its principal targets [4]. Nek1 activation depends on its phosphorylation by TLK at T141, and this in an early DDR event upstream of ATR and Chk1 upon oxidative damage or replication arrest [4], extending earlier studies on Nek1 [19]. We have now shown that preventing Nek1 activation by inhibiting TLK functions with THD results in

significant delay in the progression of the TRAMP cancer model, both in carcinogenic progression of the prostate glands and even later during NE differentiation. In addition, the expression of TLK1 and p-Nek1 was correlated with each other and with the tumor grade (GS) in the (admitted limited) number of PCa biopsies that were available to us. This suggests that the TLK1 > Nek1 axis, in addition to being a critical mediator of the DDR [1,4] may have additional functions during progression of PCa, particularly during conversion to CRPC. In fact, expression analysis Nek1 revealed upregulation in 33% of patients and gene amplification in 12% of patients with NE-CRPC. Nek1 is the first identified member in human of the NIMA family of protein kinases that was originally identified in *Aspergillus nidulans* as a protein kinase essential for mitosis [20]. NIMA related kinases (NEKs) have adapted to a variety of cellular functions in addition to mitosis [21]. In humans, 11 NEKs were identified that are involved in several functions, whereby Nek1 [22–24] and Nek4 [25] have been mostly implicated in the DDR and DNA repair pathways [26]. Nek1 promotes Chk1 activation via its association with ATR-ATRIP and primes ATR for the DDR [19], and its suppression abolishes the checkpoint and results in genomic instability [22,27]. Not all the substrates of Nek1-11 have been fully elucidated, and the majority of NEKs are involved in more than one of the three NEKs core functions: (1) centrioles/mitosis; (2) primary ciliary function/ciliopathies; and (3) the DNA damage response (rev. in Ref. [21]). Deletion mutations in the Nek1 gene in mice cause polycystic kidney disease (PKD) and other pleiotropic effects, ranging from facial dysmorphism, dwarfing, male sterility, anemia and cystic choroid plexus. The pleiotropic nature of these phenotypes suggested a role of Nek1 early on in development [28]. But even later in life, it was recently discovered that certain mutations in Nek1 confer susceptibility to development of ALS [29], all of which suggest that Nek1 may be critically involved in controlling disease progression and development. We recently uncovered the TLK1 > Nek1 axis in regulating the DDR [4] and have recently reported that its inhibition with THD results in bypass of the checkpoint response and induction of apoptosis in vitro and in xenografts [1]. However, we have now shown that the TLK1 > Nek1 axis may affect additional aspects of PCa progression, and particularly regulate CRPC and NE progression, thus offering an even more important target for development of specific inhibitors of this pathway.

Authors' contribution

Conception and design: V. Singh, P. Jaiswal, I. Ghosh, H. Koul, X. Yu, A. De Benedetti.

Development of methodology: V. Singh, P. Jaiswal, I. Ghosh, H. Koul, X. Yu, A. De Benedetti.

Acquisition of data: V. Singh, P. Jaiswal, I. Ghosh, A. De Benedetti.

Analysis and interpretation of data (e.g., statistical analysis, biostatistics, computational analysis): V. Singh, P. Jaiswal.

Writing, review, and/or revision of the manuscript: V. Singh, P. Jaiswal, I. Ghosh, H. Koul, X. Yu, A. De Benedetti.

Administrative, technical, or material support**:** V. Singh, P. Jaiswal, I. Ghosh, H. Koul, X. Yu, A. De Benedetti.

Study supervision: A. De Benedetti, H. Koul, X. Yu.

Funding

This work was supported primarily by DoD-PCRP grant W81XWH-17-1-0417 to A. De Benedetti.

Disclosure of potential conflicts of interest

No potential conflicts of interest were disclosed.

Acknowledgements

We thank Paula Polk and the Research Core Facility-Genomics and the Histopathology Core at LSU Health-Shreveport, which is supported in part by the LSU Health Shreveport Foundation, the Biomedical Research Foundation, the Center for Molecular and Tumor Virology, the Center for Cardiovascular Diseases and Sciences, and the Feist-Weiller Cancer Center (FWCC).

References

[1] V. Singh, P. Jaiswal, I. Ghosh, H.K. Koul, X. Yu, A. De Benedetti, Targeting the TLK1/NEK1 DDR axis with thioridazine suppresses outgrowth of androgen independent prostate tumors, Int. J. Cancer (2019), https://doi.org/10.1002/ijc.32200 in press.

[2] B.S. Carver, C. Chapinski, J. Wongvipat, H. Hieronymus, Y. Chen, S. Chandarlapaty, V.K. Arora, C. Le, J. Koutcher, H. Scher, et al., Reciprocal feedback regulation of PI3K and androgen receptor signaling in PTEN-deficient prostate cancer, Cancer Cell 19 (5) (2011) 575–586.

[3] R.J. DeFatta, E.A. Turbat-Herrera, B.D.L. Li, W. Anderson, A. De Benedetti, Elevated expression of eIF4E in confined early breast cancer lesions: possible role of hypoxia, Int. J. Cancer 80 (1999) 518–522.

[4] V. Singh, Z.M. Connelly, X. Shen, A. De Benedetti, Identification of the proteome complement of humanTLK1 reveals it binds and phosphorylates NEK1 regulating its activity, Cell Cycle 16 (10) (2017) 915–926 910.1080/15384101.15382017.11314421. Epub 15382017 Apr 15384120.

[5] J.R. Gingrich, R.J. Barrios, R.A. Morton, B.F. Boyce, F.J. DeMayo, M.J. Finegold, R. Angelopoulou, J.M. Rosen, N.M. Greenberg, Metastatic prostate cancer in a transgenic mouse, Cancer Res. 56 (18) (1996) 4096–4102.

[6] J.R. Gingrich, R.J. Barrios, M.W. Kattan, H.S. Nahm, M.J. Finegold, N.M. Greenberg, Androgen-independent prostate cancer progression in the TRAMP model, Cancer Res. 57 (21) (1997) 4687–4691.

[7] A. De Benedetti, The Tousled-Like-Kinases as guardians of genome integrity, ISRN Mol. Biol. 2012 (2012 Jan 1) 627596.

[8] G. Sunavala-Dossabhoy, Preserving salivary gland physiology against genotoxic damage - the Tousled way, Oral Dis. 24 (8) (2018) 1390–1398 1310.1111/odi.12836. Epub 12018 May 12832.

[9] K. Byrnes, A. De Benedetti, N. Holm, J. Luke, J. Nunez, Q. Chu, C. Meschonat, F. Abreo, L. Johnson, B. Li, Correlation of TLK1B in elevation and recurrence in doxorubicin-treated breast cancer patients with high eIF4E overexpression, J. Am. Coll. Surg. 204 (5) (2007) 925–933.

[10] S.-B. Lee, S. Segura-Bayona, M. Villamor-Payà, G. Saredi, M.A.M. Todd, C.S.-O. Attolini, T.-Y. Chang, T.H. Stracker, A. Groth, Tousled-like kinases stabilize replication forks and show synthetic lethality with checkpoint and PARP inhibitors, Science Advances 4 (8) (2018) eaat4985-eaat4985.

[11] S. Ronald, S. Awate, A. Rath, J. Carroll, F. Galiano, D. Dwyer, H. Kleiner-Hancock, J.M. Mathis, S. Vigod, A. De Benedetti, Phenothiazine inhibitors of TLKs affect double-strand break repair and DNA damage response recovery and potentiate tumor killing with radiomimetic therapy, Genes Cancer 4 (1–2) (2013) 39–53.

[12] J. Jiang, P. Jia, Z. Zhao, B. Shen, Key regulators in prostate cancer identified by co-expression module analysis, BMC Genomics 15 (2014) 1015.

[13] S. Ronald, G. Sunavala-Dossabhoy, L. Adams, B. Williams, A. De Benedetti, The expression of Tousled kinases in CaP cell lines and its relation to radiation response and DSB repair, Prostate 71 (13) (2011) 1367–1373.

[14] G. Sunavala-Dossabhoy, M. Fowler, A. De Benedetti, Translation of the radioresistance kinase TLK1B is induced by gamma-irradiation through activation of mTOR and phosphorylation of 4E-BP1, BMC Mol. Biol. 5 (2004) 1.

[15] Y. Li, R. DeFatta, C. Anthony, G. Sunavala, A. De Benedetti, A translationally regulated Tousled kinase phosphorylates histone H3 and confers radioresistance when overexpressed, Oncogene 20 (6) (2001) 726–738.

[16] J. Pelletier, J. Graff, D. Ruggero, N. Sonenberg, Targeting the eIF4F translation initiation complex: a critical nexus for cancer development, Cancer Res. 75 (2) (2015) 250–263.

[17] A. De Benedetti, J.R. Graff, eIF-4E expression and its role in malignancies and metastases, Oncogene 23 (2004) 3189–3199.

[18] M. Bhat, N. Robichaud, L. Hulea, N. Sonenberg, J. Pelletier, I. Topisirovic, Targeting the translation machinery in cancer, Nat. Rev. Drug Discov. 14 (2015) 261.

[19] S. Liu, C.K. Ho, J. Ouyang, L. Zou, Nek1 kinase associates with ATR-ATRIP and primes ATR for efficient DNA damage signaling, Proc. Natl. Acad. Sci. U. S. A. 110 (6) (2013) 2175–2180.

[20] S.A. Osmani, R.T. Pu, N.R. Morris, Mitotic induction and maintenance by overexpression of a G2-specific gene that encodes a potential protein kinase, Cell 53 (2) (1988) 237–244.

[21] G.V. Meirelles, A.M. Perez, E.E. de Souza, F.L. Basei, P.F. Papa, T.D. Melo Hanchuk, V.B. Cardoso, J. Kobarg, "Stop Ne(c)king around": how interactomics contributes to functionally characterize Nek family kinases, World J. Biol. Chem. 5 (2) (2014) 141–160.

[22] Y. Chen, P.L. Chen, C.F. Chen, X. Jiang, D.J. Riley, Never-in-mitosis related kinase 1 functions in DNA damage response and checkpoint control, Cell Cycle 7 (20) (2008) 3194–3201.

[23] Y. Chen, C.F. Chen, D.J. Riley, P.L. Chen, Nek1 kinase functions in DNA damage response and checkpoint control through a pathway independent of ATM and ATR, Cell Cycle 10 (4) (2011) 655–663.

[24] A.L. Pelegrini, D.J. Moura, B.L. Brenner, P.F. Ledur, G.P. Maques, J.A. Henriques, J. Saffi, G. Lenz, Nek1 silencing slows down DNA repair and blocks DNA damage-induced cell cycle arrest, Mutagenesis 25 (5) (2010) 447–454.

[25] F.L. Basei, G.V. Meirelles, G.L. Righetto, D.L. Dos Santos Migueleti, J.H. Smetana, J. Kobarg, New interaction partners for Nek4.1 and Nek4.2 isoforms: from the DNA damage response to RNA splicing, Proteome Sci. 13 (2015) 11.
[26] J. Spies, A. Waizenegger, O. Barton, M. Surder, W.D. Wright, W.D. Heyer, M. Lobrich, Nek1 regulates Rad54 to orchestrate homologous recombination and replication fork stability, Mol. Cell 62 (6) (2016) 903–917.
[27] Y. Chen, C.F. Chen, H.C. Chiang, M. Pena, R. Polci, R.L. Wei, R.A. Edwards, D.E. Hansel, P.L. Chen, D.J. Riley, Mutation of NIMA-related kinase 1 (NEK1) leads to chromosome instability, Mol. Canc. 10 (1) (2011) 5.
[28] P. Upadhya, E.H. Birkenmeier, C.S. Birkenmeier, J.E. Barker, Mutations in a NIMA-related kinase gene, Nek1, cause pleiotropic effects including a progressive polycystic kidney disease in mice, Proc. Natl. Acad. Sci. U. S. A. 97 (1) (2000) 217–221.
[29] K.P. Kenna, P.T.C. van Doormaal, A.M. Dekker, N. Ticozzi, B.J. Kenna, F.P. Diekstra, W. van Rheenen, K.R. van Eijk, A.R. Jones, P. Keagle, et al., NEK1 variants confer susceptibility to amyotrophic lateral sclerosis, Nat. Genet. 48 (9) (2016) 1037–1042.